Laser spectroscopic studies on scattering media

- Application to food packages and wood materials

Jim Larsson

Supervisors: Sune Svanberg and Liang Mei

Master Thesis
Spring semester, 2014
Atomic Physics

Lund University
Faculty of Science

Populärvetenskaplig sammanfattning

När ljus passerar igenom materia, så som gaser, vätskor eller fasta material, finns det en viss sannolikhet att materian absorberar delar av ljuset. Ljus som absorberas ger ett energitillskott till atomerna och molekylerna i materian. Energin som en atom eller molekyl absorberar beror på våglängden av ljuset, där en kortare våglängd motsvarar en högre energi. Bara en mycket liten del av det elektromagnetiska vågor består av är synligt för oss människor och tolkas av våra hjärnor som färger. Följdaktigen är det så att varje sorts atom och molekyl har sitt eget unika antal våglängder som de kan absorbera, vilket är en konsekvens av vårt universum och som inom fysiken förklaras med hjälp av kvantmekaniken. Absorption av ljus är den kanske viktigaste processen för liv på jorden. Det är så växternas löv kan omvandla solljuset till användbar energi i fotosyntesen, där även koldioxid omvandlas till syre.

Inom absorptionsspektroskopi använder man olika experimentella metoder för att studera de våglängder som atomer och molekyler absorberar. Genom att observera vilka våglängder som absorberas när ljuset passerar till exempel en cell fylld med gas, kan man identifiera vilka gaser det är som befinner sig i cellen. Mängden av absorberad strålning vid de olika våglängderna kan tala om hur mycket av varje ämne man har.

I detta arbete har studier baserade på absorptionsspektroskopi gjorts av gaser som är imbäddade i porerna hos spridande material, så som trä och matförpackningar. Denna speciella tillämpning av absorptionspektroskopi, har fått namnet GASMAS. Utmaningarna som uppstår när man mäter i spridande medier är att när ljuset observeras så har det färdats över en okänd vägsträcka; detta gör att det är svårare att erhålla information om gasens egenskaper, till exempel dess koncentration. För att försöka få ut mer information om de material man studerar, kombineras GASMAS med en mätmetod där man modulerar lasern så att svängningar i ljusintensitet uppstår. När man sedan låter detta ljus passera igenom ett spridande medium så kommer ett fasskift att erhållas på grund av den längre avverkade vägsträckan i mediet. Genom att sedan studera fasskiftet som uppstår kan man få information om mediets spridande egenskaper samt så kan man utvärda den optiska väglängden genom mediat.

Studier har i detta projekt dels gjorts på matförpackningar; i dessa mätningar undersöktes hurvida man på ett snabbt och tillförlitligt sätt kunde mäta koldioxidkoncentrationen i brödförpackningar. Sedan undersöktes också de optiska egenskaperna hos mjölkförpackningar genom att mäta absorption av syre i den gasfyllda överdelen av förpackningen. Mätningarna på brödförpackningarna gav en hög koncentration koldioxid och resultatet visade att med hög absorption och en bra signal kan man utföra kontrollmätningar under en tid på 50 ms per förpackning. Mätningarna utförda på mjölkpaket visade att genom att ändra konsistensen på mjölken, genom att späda ut med vatten, så påverkas samtidigt absorptionssignalen och den totala optiska vägsträckan som ljuset färdas i paketen. Detta har att göra med att ljuset färdas olika i mjölken beroende på hur utspädd den är. Detta skulle möjligtvis kunna användas för att observera förändringar i konsistens av vätskor. Absorptionssignalen från syret i en ny oöppnad mjölkförpackning var övervakad under en längre tid. Efter 7 dagar kunde en förändring i syrets absorptionssignal observeras och efter ungefär 15 timmar hade syresignalen helt försvunnit. Denna process förklarades med att bakterierna i mjölken blir aktiva och börjar konsumera syret i förpackningen. Genom att studera hur fort

och när bakterierna konsumerar syret kan man erhålla information om tillväxten av bakterier i mjölken.

Andra delen av arbetet var att verifiera en metod för att utföra mätningar på arkeologiskt trä, så som från skeppet Vasa. En svårighet att göra absorptionsspektroskopi på arkeologiskt trä är att det ofta är mycket mörkt och släpper igenom lite ljus. För att utvidga studierna utfördes istället gas diffusion mätningar i furu och mahogny genom att borra ett hål och föra in optiska fiber som är kopplade till en laser och detektor. Genom att sedan föra in kvävgas i ett närliggande hål och sen detektera hur syrets absorptionssignal i hålet med fibrerna förändras, kunde en strukturell skillnad mellan furu och mahogny observeras.

Abstract

In this project, an optical technique called gas in scattering media absorption spectroscopy (GASMAS) has been employed to investigate optical properties in scattering media such as food packages and wood materials. The GASMAS technique has been combined with a technique called frequency domain photon migration (FDPM) and from the integrated system the gas absorption signal and total optical path length have been assessed when measuring on milk packages. Measurements performed on empty packages with thin walls show that the total optical path length could be a good approximation of the gas absorption length, enabling gas concentration assessment through Beer-Lambert law in some cases. However, when a liquid is present in the package, its optical properties will affect both the absorption and total path length of the light. When performing headspace measurements on the milk package, it was shown that a decrease of the scattering coefficient in the milk resulted in a decrease in absorption path length. When replacing the milk content with water, a drastic decrease in both absorption path length and total optical path length could be observed.

The integrated system was also was used to perform a longtime study on a sealed milk package. The GASMAS measurement mode was used to take data continuously over several days and sample measurements were performed with the setup working in the FDPM mode. From the results it could be concluded that the decrease of the absorption signal was due to the depletion of oxygen in the headspace of the package and no change of the optical properties in the milk could be observed. By fitting the absorption signal to a bacterial growth formula, it was then demonstrated that the GASMAS technique can be used to indirectly monitor the bacterial population by measuring the gas content in the headspace.

The GASMAS technique was also employed for gas diffusion studies inside pine and mahogany wood samples. A fiber probe was developed consisting of two optical fibers for light delivery and collection, i.e., one fiber was coupled to the diode laser and the second one to a PMT. By inserting the probe into a hole of the wood sample and flushing with nitrogen into another hole at a distance of 10 mm, the gas diffusion process would occur. It was shown that the pine sample had a much faster gas exchange rate with the ambient air compared to the mahogany sample, providing a great potential of using the fiber probe for archaeological wood material studies.

Contents

Chapter 1

Introduction and background

This Master project is equivalent to 30 ETSC and has been carried out during the Spring semester of 2014 in the *Applied molecular spectroscopy and remote sensing group* in the Atomic Physics Division at Lund University.

Optical methods provide useful tools for many applications such as environmental monitoring [1], medical diagnosis [2], chemical analysis [3] and combustion diagnostics [4], with applications in both science and industry. Advantages of using optical methods over chemical or nuclear analysing tools include short measuring times and the possibility for non destructive measurements. These advantages are important, e.g., when doing *in vivo* experiments for medical applications.

In the group of *Applied molecular spectroscopy and remote sensing* an optical technique called GASMAS (short for Gas in Scattering Media Absorption Spectroscopy) for investigation of gas embedded in turbid media was introduced in 2001 [5], to utilize the sharp absorption features of the gas molecules, compared to the broadband absorption signature of the bulk materials. The technique is based on tunable diode laser absorption spectroscopy (TDLAS) [6], where the wavelength of the laser light from a diode laser is scanned over one of the absorption lines from the gas molecule of interest. By detecting the transmitted intensity, an absorption profile may be retrieved which holds information about the sample such as gas concentration, pressure and temperature. The amount of absorption, which is the ratio of the detected transmitted light intensity to the initial intensity before propagating through the sample, is described by the Beer-Lambert law. It states, that the transmitted light intensity is exponentially decaying as a function of the product of concentration and optical path length. In a non-scattering medium the optical path length is known by just measuring the sample and thus the concentration can be assessed. By moving to the regime where the sample under study no longer has a well defined optical path length, i.e., a scattering medium, the Beer-Lambert law can no longer be used to retrieve the gas concentration. For this special case of TDLAS, that got the name GASMAS, additional methods need to be employed to retrieve information about the path length.

In my previous Bachelor project [7], which was performed during the Spring semester of 2012 in the same research group, an experimental setup was developed which integrated two optical techniques, the GASMAS and FDPM (frequency domain photon migration) techniques. When employing the FDPM technique, the laser beam from a diode laser is intensity-modulated by a frequency in the MHz range. When propagating through a sample, the light will then obtain a phase shift. By employing a suitable light propagation model, the mean optical path length through the scattering medium

can be assessed. In previous work this combined setup has been used to investigate the porosity of porous materials [8, 9] by defining the optical porosity as the ratio between the gas absorption path length and the total path length.

In this thesis, which can be seen as a continuation of my bachelor project, scattering materials such as wood materials and food packages have been investigated using the GASMAS technique. By combining with the FDPM technique, the relation between absorption path length and total path length in food packages, where heavy scattering is present in the walls of the package and in the liquid, has been investigated. By monitoring of the absorption, information about the gas concentration inside the packages can be obtained. The main purpose of packages is to protect food from spoilage and here a proper gas concentration inside the packages has a vital role in preserving the freshness of the food. Therefore, to be able to monitor the filling gases is of vital importance with regards to assessing shelf time and prevent spoilage. Interesting gases to monitor would be oxygen, nitrogen and carbon dioxide. The oxygen gas is reactive and crucial for aerobic bacteria. In packages it is common to instead use a high concentration of carbon dioxide or nitrogen.

This thesis work is also connected to a project for archaeological wood studies, such as the wood materials from the shipwrecked Vasa ship, now on display in Stockholm. The Vasa ship is mainly made of oak, which is a very dense wood material. The project is to study and understand the structure of the oak materials. However, it is very difficult to do direct GASMAS studies on the samples because of the strong light absorption in the bulk material. Thus, a fiber probe was developed to study gas diffusion processes through wood materials, and in this part of the work the aim was mainly to verify the possibility of such a measurement technique.

The outline of the thesis will be as follows; first, following this introduction, a brief discussion of the physical principles behind absorption spectroscopy, such as the molecular energy structure and absorption is introduced, then various optical techniques will be presented. This is followed by the methods and materials used in the project and the associated results and discussion about the results. At the end the conclusions and outlook of the thesis work are given.

1.1 Molecular energy levels

Molecules are formed when two or more atoms bond together by sharing or transferring electrons, a process resulting in a lower total energy compared to the combined energy of the individual constituents. The energy state of the molecule will be characterized by the new electron configuration from the combined atoms and an additional contribution to the energy from the relative movement of the nuclei in the molecule, which is divided into vibrational and rotational motion and has a profound impact on the molecular energy structure.

Molecules exhibit a unique set of energy levels, similar as in atoms; however there is a drastic increase in complexity due to the added contribution from the rotational and vibrational components. In the simplest description, the electronic, vibrational and rotational contributions are said to be independent. The total energy is then the sum of the independent energy components (Equation 1.1). This description of the molecular energy is generally known as the Born-Oppenheimer approximation, in which the wave function of the molecule is obtained by separating it into an electronic

and a molecular part [10], and correspondingly for the energy.

$$E_{total} = E_{electron} + E_{vibration} + E_{rotation} \tag{1.1}$$

The electronic structure of the molecule can be viewed as due to interaction between the electronic orbitals from the individual atoms, where the formation of molecular orbitals gives rise to bonding and antibonding potentials [11]. In a bonding potential the nucleus will experience a potential very much like the anharmonic oscillator, often modelled by the Morse potential (Equation 1.2). In a Morse potential, with the depth, D_0, being the dissociation energy, there is a preferable internuclear distance, r_0, in the molecule for which it obtains a lowest energy, which makes it a stable energy state of the molecule. On the other hand, the antibonding potential has a minimum energy for an infinite internuclear distance and the molecular energy at shorter separations is higher than for when the atoms are separated; thus no molecule is formed. The energy separations between electronic states are similar to what is found in the atoms and usually correspond to transition wavelengths in a range from a few hundred nm to one µm.

$$E = D_0(1 - \mathrm{e}^{a(r_0 - r)})^2 \tag{1.2}$$

The vibrational motion in the molecule can be viewed as a change in bond length between the nuclei and the vibration will be restricted to the Morse potential that the molecule is experiencing. From the theory of quantum mechanics and by solving the Schrödinger equation for an anharmonic oscillator, a discrete set of solutions are obtained, corresponding to a discrete set of possible vibrational states. From the solutions it is also shown that the energy of the lowest vibrational state is non-zero and that the spacing between vibrational states decrease for higher states:

$$E_{vibrational} = (v + \frac{1}{2})w_e - (v + \frac{1}{2})^2 w_e x_e \tag{1.3}$$

Here v is the vibrational quantum number, w_e is the oscillation frequency and x_e is a constant depending on the molecule. The spacing between the vibrational states corresponds to an energy in the mid-infrared region. However, the absorption/emission of light in this region requires a change in dipole moment.

As mentioned earlier, in addition to vibration, the rotational motion will also contribute to the total energy of the molecule and, just as for vibration, there are only a discrete set of rotational states. The spacing of rotational states are much lower than that for the vibrational states (transitions in the microwave range) and will act as a fine structure to the vibrational states. For most applications, the energy resulted from the rotation is described by an non-rigid rotator in the quantum mechanical regime:

$$E_{rotational} = BJ(J+1) - DJ^2(J+1)^2 \tag{1.4}$$

Here the rotational constant, B, is inversely proportional to the moment of inertia, D is the centrifugal distortion constant and J is the rotational quantum number.

Transitions between electronic energy levels in molecules can also be followed by a change in vibration and rotational levels, which results in a complex transition profile. If the molecule interacts with electromagnetic radiation, spectral lines can be observed with an energy that corresponds to the energy needed to make a transition between two energy levels. The intensity of a transition is then related to the probability for

a transition. In a measurement the observed spectral line will have a profile broadening, which is to be discussed later. The intensity will also be dependent on how the molecules are distributed on available energy levels. The spectral fingerprint is unique to each kind of molecule, but compared to atoms the spectral lines are grouped up in what is called *bands*, which are formed due to many possible vibrational-rotational transitions.

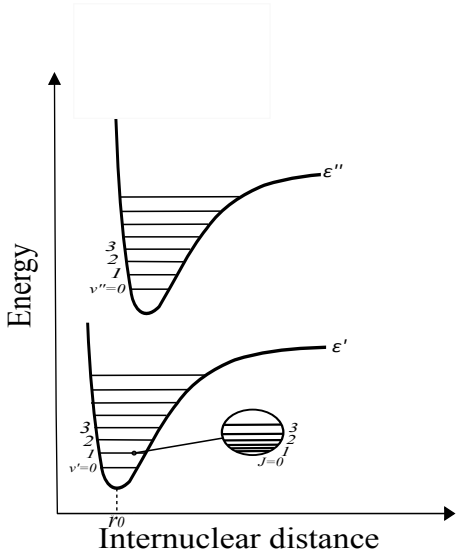

Figure 1.1: Schematic of a two-level system for a molecule. The electronic ground state, ε', and excited state, ε'', both show vibrational states, v' and v''. Zooming in on a vibrational state reveals rotational states, J, due to the rotational movement of the molecule.

1.2 Line broadening

The spectral lines will have a finite width, which is caused by several broadening mechanisms. The line profile is usually characterized by its value for the half width at half maximum (HWHM) and the most important contributions are natural, Doppler and pressure broadening.

Natural broadening occurs from the finite lifetime, τ, of the energy states and a shorter lifetime will give rise to larger broadening, $\Delta\nu_{natural}$:

$$\Delta\nu_{natural} = \frac{1}{2\pi\tau} \tag{1.5}$$

The above equation is directly related to the uncertainty principle, which states that there is a limit on how accurately time and energy can be measured simultaneously. The implication of this is that there is a natural limit which prevents energy levels with infinitesimal line width.

Doppler broadening arises from the thermal motion of the molecules. The line profile caused by Doppler broadening is described by a Gaussian and the broadening is dependent on the temperature, T, and mass, M, of the particles:

$$\Delta\nu_{doppler} = \frac{2\sqrt{2k\ln 2}}{c}\nu_0\sqrt{\frac{T}{M}} \tag{1.6}$$

Here k is the Boltzmann constant and ν_0 is the central frequency when the molecules do not move. Doppler broadening is an inhomogeneous broadening, where the Doppler shift for each particle is individually contributing to the whole broadening profile.

Pressure broadening comes from collisions between the particles. Collisions will distort the energy levels and by quenching increase the decay rate of the excited state, thus reducing the lifetime, which gives rise to broadening. As the name implies, the pressure broadening is dependant on the pressure, P, and temperature:

$$\Delta\nu_{pressure} = \Delta\nu_{P_0,T_0}\frac{P}{P_0}\sqrt{\frac{T_0}{T}} \tag{1.7}$$

Here $\Delta\nu_{P_0,T_0}$ is the pressure broadening at room temperature and atmospheric pressure, having a Lorentzian profile with a HWHM of about 1-5 GHz. The total contribution of the broadening mechanisms are included in the Voigt profile, which is retrieved by taking the convolution of the individual line profiles.

1.3 Absorption

When electromagnetic radiation, light, passes through a gas of molecules or atoms there is a probability that the light will be absorbed. When the light is absorbed, the absorbing particle will be transferred to a higher energy state, which corresponds to the added energy of the absorbed light. From the discrete nature of the energy states of atoms and molecules it follows that no absorption will occur if the energy of the light is not equivalent to the separation between two energy levels. To explain the absorption process, light is described as a quantized particle and this light particle is called a *photon*. The theory of light being particles instead of waves was introduced in the early 20th century and was successfully employed when it could explain the "ultraviolet catastrophe" [12] and the photoelectric effect [13]. This was achieved by identifying the energy of the photon as being proportional to the frequency of the light, $E = h\nu$, where the scaling constant, h, is called Planck's constant. Before the breakthrough of the particle model, the light was described as a pure wave with an energy related to the amplitude of the wave. Today light is described to have both particle and wave properties depending on how it is observed.

The probability that a photon and a quantized molecular system interact through absorption is described by, σ, the absorption cross section, which is dependent on the molecule and the wavelength of the light. For light propagating through a medium, the absorption will also be dependent on the propagation path length, l, and the concentration, c, of absorbers. The transmitted light intensity, I, through an absorbing medium is exponentially decaying as described in the following relation, were I_0 denotes the intensity of light before absorption:

$$I = I_0 e^{-\sigma c l} \tag{1.8}$$

This relation is known as the Beer-Lambert law and it assumes that the absorption of the photon in the medium is a homogeneous and random process, and that the absorption events are independent. These conditions are similiar to the definition for a Poisson distribution [14].

Broadening mechanisms of spectral lines make it possible for molecules to absorb photons slightly off the resonance wavelength. For gas molecules the width of the

spectral line is very narrow, only broadened by the Doppler effect and pressure effects. However, this is not the case for molecules in liquids or solids where the energy levels are heavily perturbed by the surrounding molecules. The absorption in liquids and solids has broad profiles, very different from the narrow gas absorption lines observed in, e.g., GASMAS. As an observation there also exist non-linear absorption processes such as two-photon absorption, where the photon energy does not need to satisfy the energy needed for a transition; rather, the sum of the two photon energies corresponds to the transition.

1.4 Light propagation in turbid media

In turbid media there are two processes which describe its optical properties, absorption and scattering. As discussed earlier, absorption can occur due to the energy of the light coinciding with a transition of the gas molecules, or it can be absorbed by the bulk material. To describe the absorption it is common to use the absorption coefficient, μ_a, which has a unit of inverse centimetre and is the reciprocal of the mean free path of the photon before an absorption event occurs. In a similar way, the scattering coefficient, μ_s, is defined. Again, the unit is inverse centimeter and the reciprocal is the mean free path before the photon encounters a new scattering event.

In a homogeneous medium the incident light is scattered in all directions; however, if the medium holds an orientation dependent structure then the scattered intensity profile will be dependent on the incident light. In scattering theory this is expressed with the anisotropy factor [15]:

$$g = \int p(\theta)\cos(\theta)\mathrm{d}s' \tag{1.9}$$

which is the mean value of the cosine of the scattering angle, θ, and $p(\theta)$ is a phase function. So as an example, an anisotropy factor of zero corresponds to a completely random scattering and a high value of g means that the incident light will experience a forward oriented scattering. The anisotropy factor is usually used to define a new coefficient, the reduced scattering coefficient, $\mu_s' = (1-g)\mu_s$. The above parameters are then used to model light propagation in turbid media and can be done as treating the light as photons in the radiative transfer equation, solved by either the diffusion approximation [16] or the Monte Carlo method [17]. For analysis of experimental data, light propagation models can be employed to solve the inverse problem of having a sample with unknown properties. This requires that the models can describe the sample, such as employing suitable boundary conditions to describe the geometry of the sample.

Chapter 2

Spectroscopy

2.1 Tunable diode laser absorption spectroscopy

Two years after the introduction of the laser in 1960, the first diode laser was demonstrated [18] using gallium arsenide as a semiconductor material. Not long after this the first diode laser that could operate in continuous-wave mode was demonstrated [19]. The diode laser was then successfully employed in measuring absorption spectra [20] with high-resolution and good tunability, which is difficult with conventional light sources and, at that time available gas lasers. The method of doing absorption spectroscopy using diode lasers is called, as mentioned in Chapter 1, tunable diode laser absorption spectroscopy (TDLAS) and is today a well developed tool for gas sensing and monitoring. TDLAS has been used to measure small concentrations of trace gases e.g., nitrogen dioxide [21], methane [22], atmospheric oxygen [23] and ammonia [24].

The principle behind TDLAS is, as previously mentioned, to use a diode laser to probe an absorption line and then to record the decrease in intensity (Figure. 2.1). Generally the laser is tuned through the injection current and the scanning range of the laser wavelength is, at least, covering one absorption line from the gas of interest. Changing the injection current of the laser will affect the properties of the semiconductor material, leading to a change in lasing wavelength accompanied by a change in the output intensity. In Equation 2.1 the observed intensity is described with the previous mentioned Beer-Lambert law, where $A(v) = c\sigma(v)$ is the absorption coefficient of the absorption line, and L is the absorption path length:

$$I(v) = I_0(v)e^{-A(v)L} \tag{2.1}$$

For small amounts of absorption, $A(v)L << 1$, the above equation may be approximated with the first order in the Taylor expansion $\exp(-A(v)L) \simeq 1 - A(v)L$:

$$I(v) \simeq I_0(v)(1 - A(v)L) = I_0(v) - I_0(v)A(v)L \tag{2.2}$$

Thus, the accuracy of measuring the absorption, $A(v)$, is then dependent on how well the difference $I_0(v) - I(v)$ of the two large signals can be measured. In the case of small absorptions, fluctuations of the intensity can heavily influence the absorption measurements and make it difficult to obtain the direct absorption signal. As a result, complementary techniques have been developed to increase the sensitivity and accuracy of TDLAS, such as frequency modulation and cavity enhanced absorption techniques. The idea is to either increase the absorption or decrease the background signal, which

in intracavity absorption is done by increasing the absorption path length, L, or as in the frequency modulation techniques where the absorption signal is detected at a much higher frequency to reduce the $1/f$ noise. In this project a modulation technique called wavelength modulation spectroscopy (WMS) has been used to enhance the small absorption signal.

Additionally to the concentration, other properties can be evaluated when performing data analysis of the retrieved absorption profile. By investigating the broadening of the absorption line, properties such as temperature and pressure can be evaluated. Furthermore, the over-all Doppler shift of the absorption signal could be used to estimate the velocity of flowing molecules.

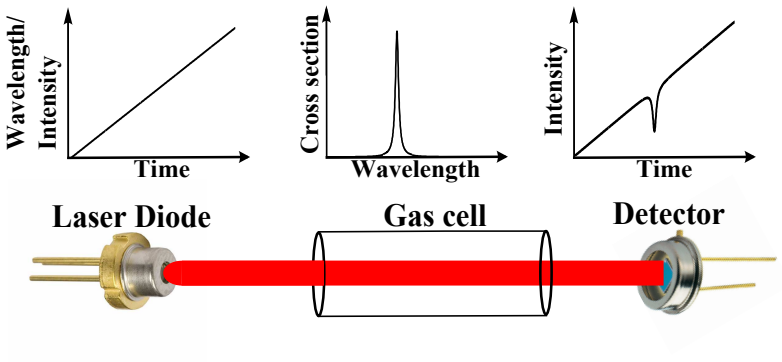

Figure 2.1: Working principle of tunable diode laser absorption spectroscopy.

2.1.1 Gas in scattering media absorption spectroscopy

When applying TDLAS on scattering porous materials which have gas filled pores embedded, and probing the gas molecules, a much more narrow absorption signal is obtained compared to the broadband signature of the bulk material. This subfield of TDLAS has its own name, GASMAS, which is short for gas in scattering media absorption spectroscopy and is treated separately because of specific challenges and solution approaches.

The absorption profile obtained from the gas molecules in a scattering material can not easily be used to evaluate the gas concentration from the Beer-Lambert law. In standard TDLAS, performed in a non-scattering sample, the gas concentration is evaluated by measuring the intensity and knowing the absorption path length which is normally equivalent to the sample length. However, when performing measurements on gas enclosed in scattering media (GASMAS), the absorption path length is not equivalent with the sample length but is instead the optical path length through the pores, and this gives rise to an unknown path length in Equation 2.1.

To relate the absorption strength and the path length in scattering media, an alternative parameter is defined, which is called *equivalent mean path length*. This is a measurement of the length the light needs to travel in a reference gas to experience the same absorption as measured through the sample. In samples which hold the same properties as the reference gas, the measured equivalent mean path length then corresponds to the mean absorption path length through the pores. As a remark it is important to note that the absorption path length is not the same as the optical path length through the scattering material, as the path through the bulk material

is not accounted into the absorption path length. The mean absorption path length is typically measured when both the reference and sample measurement is exposed to ambient air.

There are mainly two methods which have been employed to retrieve the equivalent mean path length, namely standard addition and fitting methods. In the standard addition method the sample is measured by adding known paths of free air, this will give a linear relationship between absorption signal and absorption path length that then is extrapolated to a zero absorption signal in which the equivalent mean path length is obtained. The other method, which has been used in this thesis, is to measure a reference signal with a known path length and fit the reference signal to the absorption signal measured through the sample (Equation 2.3a). Then the fitting coefficient is used to get the equivalent mean path length (Equation 2.3b).

$$Abs_{eq} = k * Abs_{ref} \tag{2.3a}$$

$$L_{eq} = k * L_{ref} \tag{2.3b}$$

The GASMAS technique has in previous work been used to study heavy scattering materials such as apples [25], ceramics [26], polystyrene foams and wood materials [8], which all are porous materials containing gas molecules. The amount of pores in a material is usually described by the porosity of the sample, defined as the ratio between the volume of the void space and the total volume of the sample.

2.2 Modulation techniques

For low absorptions or when a large amount of noise is present it can be nearly impossible to observe the absorption from the directly detected signal. In these cases signal processing techniques may be applied to suppress the noise. *Wavelength modulation spectroscopy* (WMS) and *Frequency modulation spectroscopy* (FMS) are two commonly employed modulation techniques in absorption spectroscopy. In this section the WMS will be discussed; however, it should be mentioned that both techniques have a similar approach and they differ in the choice of modulation frequency.

The principle behind WMS/FMS is that by moving the detection of the signal to a high modulation frequency the technical noise, also known as the $1/f$ noise, is significantly decreased. The wavelength modulation is accomplished by modulating the injection current through the laser driver. The laser beam which now carries an extra modulation is transmitted through a sample where some of the light is absorbed by the sample molecules. The beam intensity is then detected and the signal is then sent for processing. This procedure can be carried out either analogously with a so-called lock-in amplifier or digitally, by sampling and performing Fourier analysis on the data.

2.2.1 Wavelength modulation spectroscopy

WMS is sometimes also called derivative spectroscopy, which is based on the fact that the shape of the WMS signal resembles the derivatives of the absorption signal. In this section the theory behind the WMS signal generation when detected by a lock-in amplifier will be treated.

A lock-in amplifier, which is a phase sensitive detection device, is used to detect a signal at a certain frequency. An input signal is multiplied with a reference signal with

a certain frequency and then the resulting signal is integrated over time, which at least covers one period of the reference frequency. Input signals with frequencies not equal to the reference one will result in a zero-value net signal. Only if the frequencies of the input and reference signals are the same, an output DC signal will be obtained. This method is also phase sensitive so that a maximum output is obtained when the two signals are in-phase. If both signals are separated by a phase of 90° the output signal will be zero. The following derivation of the WMS signal holds only for sufficiently small frequency and amplitude modulations, however it give a good understanding of the physical origin of the WMS signal.

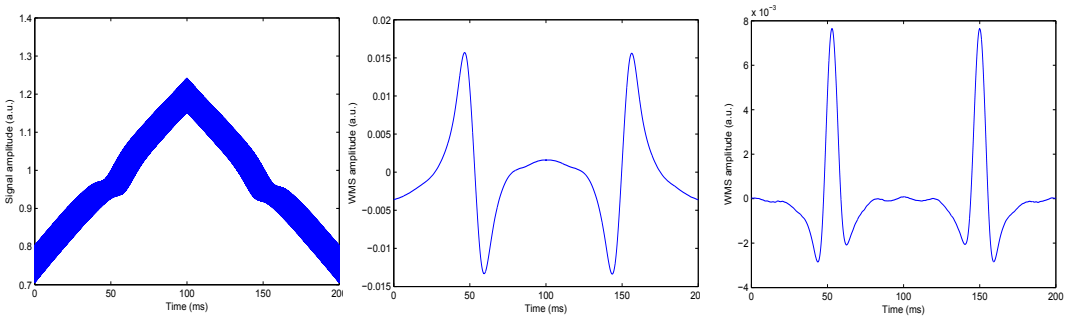

Figure 2.2: From left to right: Absorption signal measured in 38 mm polystyrene foam, with the following $1f$ and $2f$ signal obtained with Fourier analysis.

A laser is frequency modulated f_{mod} with an modulation amplitude a around its centre frequency v_c:

$$v(t) = v_c + a\cos(f_{mod}t) = v_c + \triangle v \tag{2.4}$$

The transmitted and detected intensity from the laser through a sample can be expanded in a Taylor series:

$$I(v(t) = v_c + \triangle v) = I(v_c) + \frac{\mathrm{d}I}{\mathrm{d}v}\triangle v + \frac{1}{2}\frac{\mathrm{d}^2 I}{\mathrm{d}v^2}\triangle v^2 + ... \tag{2.5}$$

By substituting $\triangle v$ with $a\cos(f_{mod}t)$ the following expression will be obtained:

$$I(v(t)) = I(v_c) + \frac{\mathrm{d}I}{\mathrm{d}v}a\cos(f_{mod}t) + \frac{1}{2}\frac{\mathrm{d}^2 I}{\mathrm{d}v^2}(a\cos(f_{mod}t))^2 + ... \tag{2.6}$$

$$= I(v_c) + \frac{\mathrm{d}I}{\mathrm{d}v}a\cos(f_{mod}t) + \frac{1}{4}\frac{\mathrm{d}^2 I}{\mathrm{d}v^2}a^2(1 + \cos(2f_{mod}t)) + ... \tag{2.7}$$

Then, by using a lock-in amplifier to detect the signal at $2f_{mod}$ with a reference signal of $\cos(2f_{mod}t)$ the signal output $S_{2f_{mod}}$ will be:

$$S_{2f_{mod}} = \frac{1}{T}\int_0^T I(v(t))\cos(2f_{mod}t)\mathrm{d}t \tag{2.8}$$

$$= \frac{1}{8}\frac{\mathrm{d}^2 I}{\mathrm{d}v^2}a^2 \tag{2.9}$$

Finally, from Eq. 2.2 and assuming a frequency independent background signal we end up with:

$$S_{2f_{mod}} = -\frac{La^2}{8}\frac{\mathrm{d}^2 A(v)}{\mathrm{d}v^2} = -\frac{cLa^2}{8}\frac{\mathrm{d}^2\sigma(v)}{\mathrm{d}v^2} \tag{2.10}$$

Here we see why WMS sometimes also is called derivative spectroscopy. However, it is worth to remark that when looking at the Taylor expansion, the nf_{mod} signal will obtain contributions from higher order terms and that this derivation is only approximative for sufficiently small modulation amplitudes.

In a more robust presentation of the WMS signal, the theory of Fourier transforms are employed and extensive studies have been performed on both the origin and the shape of the WMS signal [27].

Chapter 3

Frequency Domain Photon Migration

The frequency domain photon migration (FDPM) technique employs a sinusoidal intensity modulated light source, with a frequency that can range between a few MHz to hundreds of MHz. After passing through a sample, the detected amplitude and phase shift can be used to retrieve the scattering, μ_s, and absorption, μ_a, properties of the sample. This is usually done by analysing the phase shift and amplitude in the diffusion equation or Monte Carlo simulations. It is the scattering and absorption events in the sample that give rise to the phase shift and changed modulation depth of the intensity-modulated light. Light detected which has passed through a scattering medium has propagated in many different paths, leading to that the observed signal is an average sinusoidal signal with contribution from many different waves with different phase shifts. This also means that the obtained phase shift is related to the *mean optical path length* through the sample.

To retrieve the mean optical path length, L_{MOPL}, the measured phase shift is used together with light propagation models. However, as the boundary conditions needed in the solution are dependent on the geometry of the sample, there are not always models available for more complex geometries. For these cases a linear approximation (Equation 3.1), which has been employed in this thesis work, between phase shift (ϕ) and the mean optical path length is used instead, where c is the speed of light in vacuum. The approximation is more valid for low modulation frequencies (f_{mod}) as is demonstrated in a measurement through 38 mm polystyrene foam and shown in Figure 3.1.

$$L_{MOPL} = \frac{\phi c}{2\pi f_{mod}} \tag{3.1}$$

In order to extract the phase shift from the signal wave, detection schemes are employed that detect the phase shift in a suitable way. In the case of FDPM, the high frequencies involved are not suitable for the electronics to sample. Therefore, detection techniques such as homodyne and heterodyne detection are employed which before sampling transform the signal to a lower frequency without losing information on the phase. In this project the heterodyne detection scheme has been employed and is explained in the next section.

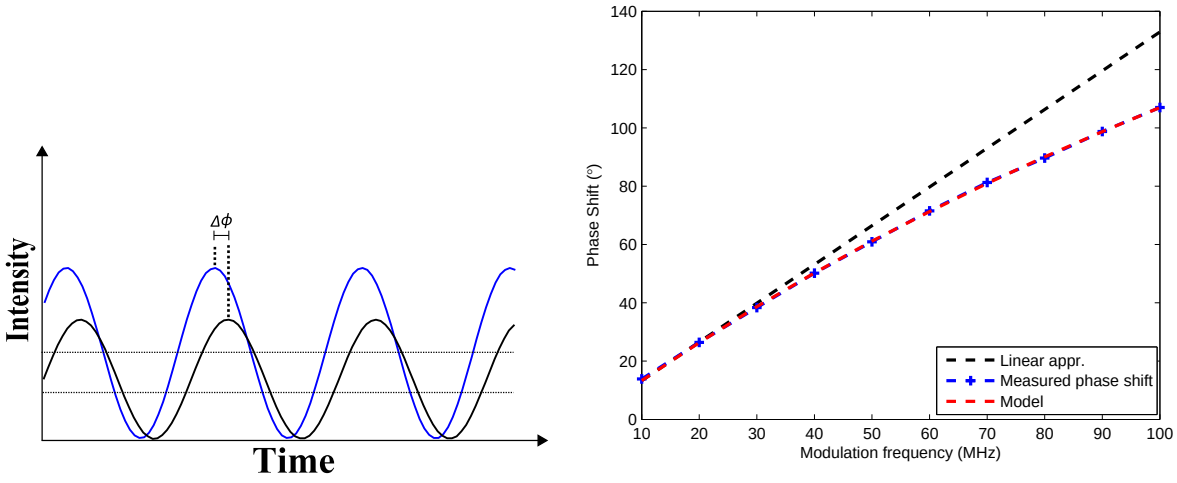

Figure 3.1: In the figure to the left, the obtained phase shift and decrease in modulation depth is demonstrated between the signal (black) and reference (black). To the right the phase shift as a function of modulation frequency is shown, and the measured phase shift is compared to the phase shift retrieved from a light propagation model and the linear approximation (Equation 3.1)

.

3.1 Heterodyne detection scheme

There can be cases where it is desirable to move the frequency of a signal to a higher or lower frequency. Such a procedure can be done by applying a heterodyne technique, which by nonlinear components generates new frequencies. In systems with very high frequencies, a down conversion may be needed for the electrical circuits to be able to handle the signal. Heterodyne techniques are used in all modern TV and radio receivers.

A component that, by a nonlinear process, can generate the new frequencies at $f_1 + f_2$ and $f_1 - f_2$ is called a mixer. A mixer can be constructed from several components, including vacuum tubes, transistors and diodes. The basic principle for all of them is that when the circuit receives two inputs, one is the signal and the other one a local oscillator, there will be a nonlinear response. The nonlinear response can be investigated by expanding the function into a power series:

$$F(v) = a_1 v + a_2 v^2 + a_3 v^3 + a_4 v^4 + ... \tag{3.2}$$

By examining the second term using the fact that the signal from the input and local oscillator is $v = A_1 \sin(f_1 t) + A_2 \sin(f_2 t)$ we obtain

$$\begin{aligned} a_2 v^2 &= a_2 (A_1 \sin(f_1 t) + A_2 \sin(f_2 t))^2 \\ &= \frac{a_2}{2}(A_1^2(1 - \cos(2f_1 t)) + A_2^2(1 - \cos(2f_2 t)) \\ &+ A_1 A_2(\cos(t(f_1 + f_2)) - \cos(t(f_1 - f_2)))) \end{aligned} \tag{3.3}$$

From the second-order term the desired mixing frequencies are generated, but harmonics of f_1 and f_2 are also produced. In addition, contributions from higher orders in (3.2) will generate higher harmonics and intermediate frequencies. An ideal mixer only

generates signals of the sum and differential frequencies. The sum-frequency signal, which has a very high frequency, is eliminated by using a low-pass filter.

Chapter 4

Materials and methods

4.1 Instrumentation

4.1.1 Experimental setup

A combined setup of the GASMAS and FDPM techniques has been used in the studies performed. It uses a semiconductor diode laser (LD-0760-0040-DFB-1,Toptica) with a lasing wavelength around 760 nm. The laser is mounted on a thermoelectric cooler (TCLDM3, Thorlabs) and is controlled through a combined temperature and current controller (ITC 502, Thorlabs). In the GASMAS setup, the laser diode is wavelength modulated by a 5 Hz sawtooth function and a 9.025 kHz sinusoidal signal. The signals are generated by a data acquisition (DAQ) card, which is a unit in the computer, and are then fed to the laser driver to modulate the laser through the injection current through a bias tee. Additionally, a fiber is coupled to the laser for increased flexibility. For detection of the light emerging from the sample, a photomultiplier tube (PMT) is used. Before the signal is sampled with a DAQ card it is amplified through a current amplifier (HCA-100M-50K-C), which in addition to amplification also transforms the current signal to a voltage signal. The sampled signal is then processesd by digital WMS and the $2f$ signal is compared to a reference signal measured with a known path length of 810 cm in ambient air.

When the setup is switched to the FDPM mode, the laser is intensity modulated by a RF generator with a frequency of 10-100 MHz, which is directly injected to the laser. The detected signal from the PMT is, through a switch (ZASWA-2-50DR+), directed to the heterodyne detection scheme previously mentioned. The detected signal is sent to a mixer after passing through a pre-amplifier (ACA-2-37-1). In the mixer the signal is demodulated to 20 kHz by using a second RF source as a local oscillator with a signal frequency carrying a 20 kHz offset. A low pass filter is used after the mixer to filter the sum-frequency signal. Finally, the signal is sampled by the DAQ card. To obtain a phase shift, a reference signal is measured by taking the signal output from the RF generator and demodulating the signal through a mixer, with the same local oscillator used for the detected signal. As just mentioned, the demodulated signal is selected through a low-pass filter and then sampled by the DAQ card. The phase shift is then assessed digitally by a procedure called the in-phase quadrant demodulation method.

The phase shift measured will also contain an offset from electrical components referred to as instrumental response. This instrumental response is measured without

the sample but with the same voltage over the PMT. The laser light is attenuated by using optical density filters, and because of amplitude-phase crosstalk the signal has to be attenuated to an amplitude which is comparable to the attenuation of the sample.

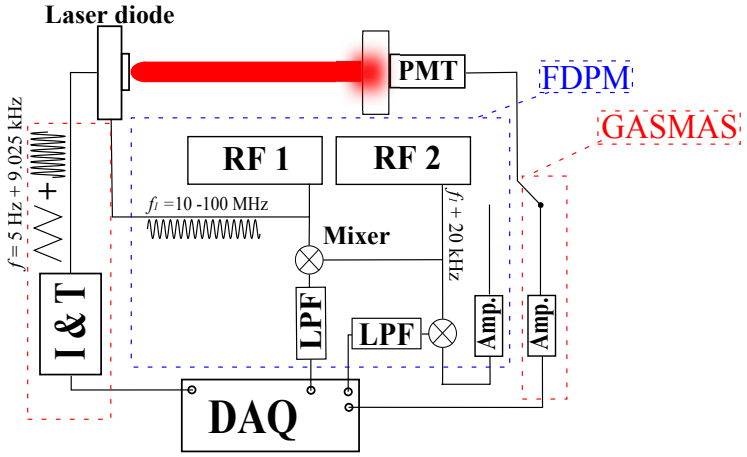

Figure 4.1: Schematic drawing of the experimental setup combining the GASMAS and FDPM technique. The two difference modes are selected by choosing modulation source and switch to the respective detection scheme. The electronic components in the setup are, photomultiplier tube (PMT), radio frequency generators (RF), low-pass filters (LPF), current and temperature controller (I & T), amplifiers (Amp.) and a data acqusition card (DAQ).

4.1.2 Evaluation of measurement errors

From the earlier work done using the combined setup of the GASMAS and the FDPM techniques [7] it was evident that the experimental system has its limits when measuring small distances. In the GASMAS mode, one limitation is interference effects which if not cancelled out completely will contribute to the WMS signal. We also have errors from absorption in free air, introduced for example between optical components. However, this can be calibrated by estimating the distance or measuring a sample with a known absorption. In the FDPM measurement and for measurements of small phase shifts, a relatively big error is introduced when performing the reference measurement of the phase shift. As mentioned in the text, all components will contribute to the measured phase shift and it is this phase shift that is measured in the recordings. The challenge of the setup arises from that the PMT gives rise to a phase shift that is dependant on both the PMT voltage and the detected intensity. For instance, by applying Equation 3.1, a difference in a phase shift of 0.2° at 10 MHz modulation frequency is roughly equivalent to a path length of 20 mm, which can be a huge difference when measuring small optical path lengths.

4.1.3 Evaluation of the *equivalent mean absorption path length*

As has been mentioned, one method to obtain an equivalent mean absorption path length (L_{eq}) is to fit an absorption signal to a reference signal measured in known conditions. With the experimental setup presented in the previous section, a reference signal was measured in air over a distance of 810 mm. The WMS signal from the

measured sample is then compared to the WMS signal of the reference (Equation 4.1). To account for changes in shape and drift of the WMS signal, a second order polynomial function is included in the fitting for which each point, t, of the WMS signal are fitted non-linear to the reference signal. From the fit, the scaling factor, c_4, is used to retrieve the equivalent mean absorption path length, $L_{eq} = c_4 * L_{ref}$.

$$WMS_{sig} = c_1 + c_2 t + c_3 t^2 + c_4 WMS_{ref} \tag{4.1}$$

In cases when the absorption signal obtains an extra contribution from outside the sample, the *equivalent mean absorption path length* has to be calibrated in regard to this offset path length.

4.2 Materials

4.2.1 Food packages

Food packages involved in the measurements were bread and milk packages, which are packaged with the so-called MAP (Modified Atmosphere Packaging) technique. The MAP technique is used to change the gas mixture inside the package to increase the shelf time. The technique gains popularity because food with no preservatives can instead be packed with an altered atmosphere and still keep its freshness for a longer time. The atmospheric composition is usually replaced with a high concentration of carbon dioxide or nitrogen, or both [28]. The exact concentration mixture is dependent on the product and a wrong concentration can result in a decrease of the shelf time. Products being packaged with the MAP technique include bread, meat, fruits and liquids such as milk.

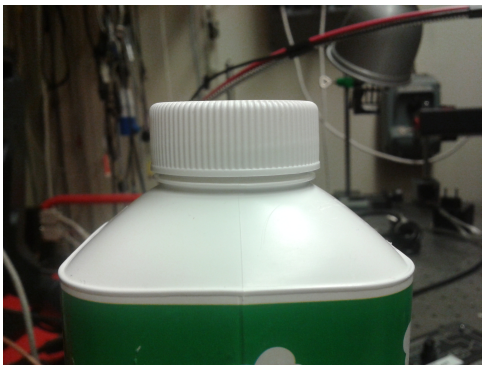

Figure 4.2: Picture of the headspace part of a milk package, which is made of plastic. The main body of the package, which in the picture is covered by colorful decoration, is made of paper.

4.2.2 Wood materials

Wood materials consist of a complex structure, with characteristics such as being porous, anisotropic and heterogeneous. Wood is commonly used as a construction material and also as a fuel. For such a widely used material it is important to understand its properties [29]. For instance, in the construction industry, the wood drying process is crucial to the resulting wood quality [30]. The wood structure determines properties

such as gas exchange and water conductivity, which are two important functions of living wood. In this work, wood samples from pine and mahogany have been used, with an estimated density of $0.4 \cdot 10^3$ kg/m^3 and $0.5 \cdot 10^3$ kg/m^3 respectively.

Figure 4.3: Picture of the cross section from a pine sample (top) and from a mahogany sample (bottom). The two wood samples show completely different structures.

Chapter 5

Measurements, Results and Discussion

5.1 Food package studies

5.1.1 CO_2 monitoring in bread packages

Two transparent bread packages were measured in a transmission mode through the air inside the package by a laser diode with a lasing wavelength close to 2 µm, probing the carbon dioxide inside. As the atmospheric concentration of carbon dioxide is less than 0.05%, the measured path length outside of the sample (offset) was neglected during data analysis. It was also assumed that when the light passes through the transparent package walls the scattering is negligible. Following the previous assumption, the optical path length of the samples could then be estimated to 90 mm and 102 mm. Absorption spectroscopy was performed on the packages by scanning the diode laser around one of the absorption lines of carbon dioxide at 2 µm by a repetition rate of 40 Hz.

From the retrieved intensity profile, the direct absorption signal could be used to evaluate the concentration of carbon dioxide inside the package; therefore WMS was not employed. From previous knowledge the package had a modified atmosphere with a concentration of carbon dioxide around 70%. To get the absorption depth from the detected signal, the measured signal was normalized by using the off-absorption line wavelengths to fit a line corresponding to the light transmitted through a non-absorbing sample. Then, using the relation in Equation 2.1 the absorption profile is obtained. Finally to evaluate the concentration, the absorption of carbon dioxide over a known path length and with a known concentration can be measured. In this case the reference was measured with a 10 cm gas cell containing 100% CO_2.

$$-\log(I/I_0)_{max,ref} = c_{ref} * L_{ref} * \sigma(\lambda) \tag{5.1}$$

$$-\log(I/I_0)_{max,sample} = c_{sample} * L_{sample} * \sigma(\lambda) \tag{5.2}$$

Here $log(I/I_0)_{max}$ is the peak value of the obtained absorption profile, c_{ref} is the concentration in the reference cell and c_{sample} is the unknown concentration in the sample, L is the path length and $\sigma(\lambda)$ is the absorption cross section. With the two above equations the unknown concentration of the sample can be found:

$$c_{sample} = \frac{\log(I/I_0)_{max,sample} * c_{ref} * L_{ref}}{\log(I/I_0)_{max,ref} * L_{sample}} \tag{5.3}$$

At a fixed position of the 90 mm package, the absorption was measured for integration times between 50 ms and 2.5 s. The results give a consistent concentration of around 64.5% CO_2 for all measuring times as shown in Figure 5.1c. The system was also investigated by measuring on several different positions on the same package to study the stability of *in situ* measurements. This was done by slightly moving the sample after each measurement and trying to keep the same path length. The integration time was chosen to 50 ms and corresponds to two times averaging. Both samples show a consistent concentration, the 90 mm sample with around 63 % carbon dioxide and the 102 mm sample with 70%, the 102 mm package displays a larger fluctuation than the 90 mm sample. As no properties inside the sample or in the system are changed; the somewhat inconsistent concentration variations originate from the challenge to reproduce the same length when changing position. The fluctuation in the concentration in Figures 5.1a and 5.1b is most likely due to the estimation of the length of the sample. It may also be that the gas concentrations are different in the two different packages.

The measurement performed on the bread packages demonstrate the possibility of using a compact setup to monitor the CO_2 content in food packages. In the packaging industry, the non destructive nature of optical techniques could be a great advantage for on-line monitoring, and each package could be checked. As already elaborated on, the main challenges for obtaining the concentration with good precision is to be able to accurately estimate the path length.

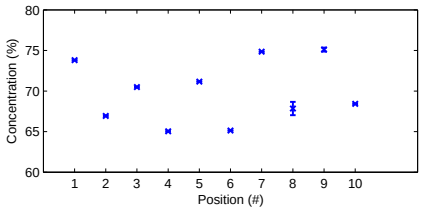

(a) 102 mm sample

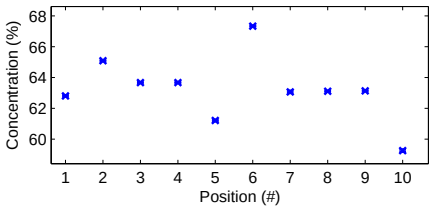

(b) 90 mm sample

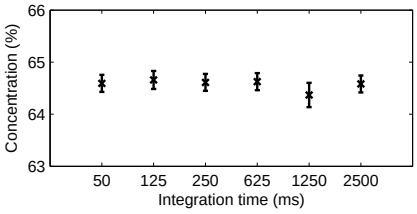

(c) 90 mm sample

Figure 5.1: (a) Concentrations of CO_2 as measured in a sample with length 102 mm. (b) Concentration retrieved from the same kind of package but 90 mm instead. (c) Concentration measured over a distance of 90 mm, but with fixed position and different integration times. The error shown in (c) arise from noise in the observed intensity, which produce an uncertainty in the data analysis. In (a) and (b) the errors are too small to be visualized as errorbars, when having errors below 0.5%.

5.1.2 Path length evaluation in milk packages

Transmission measurements were performed on milk package made of paper with a thickness of 0.5 mm (Figure 5.2). Both the GASMAS and FDPM measurements were

done by changing the distance between the two paper layers in free air, with a fiber coupled to the laser source on the first layer and the detector attached to the second layer. The distance in air between the paper layers was varied between 40-60 mm in steps of 10 mm, simulating packaged with different thickness. The measured oxygen absorption and total optical path lengths were found to match the physical path length, as shown in Figure 5.2. However, when the transmission measurements were performed through an empty, intact, package with a thickness of 71 mm, the absorption and total path length do not longer match the physical path length. The possible reason is that this could be mainly due to the reflections between the walls of the package, which then increase both the absorption and total optical path length.

In the case for the GASMAS measurement, a relative big spread with a standard deviation of 10 mm is obtained for the low distances. Factors affecting the accuracy could be disturbance from interference effects, arising from reflections in the sample and between optical components, and the fitting procedure of the WMS signal.

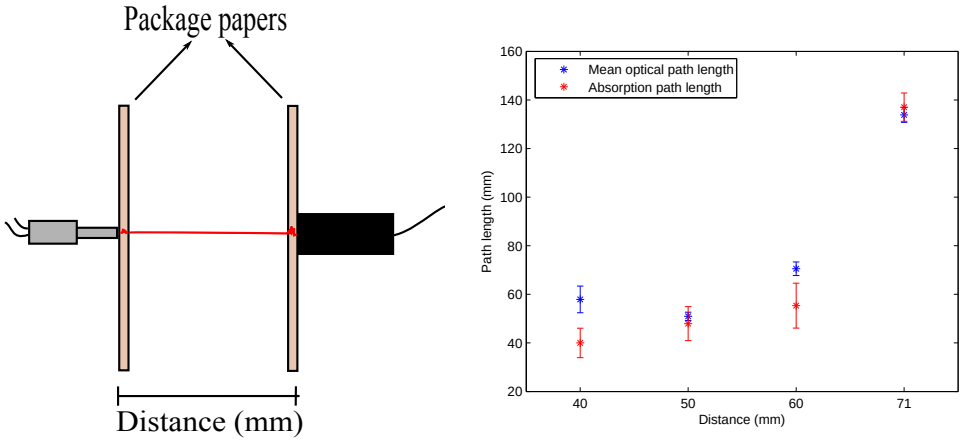

Figure 5.2: To the left a schematic drawing of the setup is shown. To the right, the GASMAS and FDPM measurements done for different distances of free air in between the package layers are presented where in GASMAS mode an absorption line of oxygen was monitored. The measurement at 71 mm was done in a enclosed milk package and the other distances were performed using two separated package layers, as is shown in the left figure.

5.1.3 Headspace measurement of milk packages

With the GASMAS/FDPM setup, headspace measurements were performed on the milk package with a top section made of plastic (Figure 5.3). The fiber and detector were placed on opposite sides, in connection to the walls, and due to the construction of the package they had to point slightly downwards into the package. The setup was tested by changing the position of the laser coupled transmitting fiber in both the GASMAS and FDPM modes. In the case of measuring the phase shift all positions of the fiber gave the same intensity for a given PMT voltage, so a single reference measurement could be used. In Table 1, the results are presented for measurements on a package containing milk and which was opened. From the results we can conclude that a slight change in position of the fiber is negligible on the outcome. When the laser light propagates through the plastic wall of the headspace, scattering will make

the light very diffuse and light will propagate in all directions inside the headspace of the milk package. This will make the detection less sensitive to the origin of the light source, as shown in Table 5.1.

Table 5.1: Measurement on different positions on the package headspaces in both GASMAS and FDPM mode. L_{eq} is the oxygen absorption path length and L_{MOPL} is the mean optical path length.

Position	L_{eq}(mm)	L_{MOPL}(mm)
1	140±4	247±3
2	146±3	247±5
3	141±2	245±3

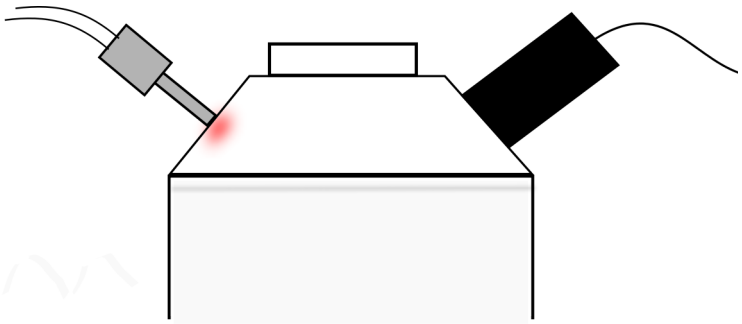

Figure 5.3: Schematic drawing of the setup when measuring the headspace content. To left the fiber is seen coupled to the laser diode and to the right of the package, the PMT is attached to the wall of the package.

The mean optical path length and the absorption path length in the headspace of a milk package were measured for different milk concentrations (Figure 5.4) to further study the possibility of using the combination method of the GASMAS and the FDPM techniques for real food packages monitoring. Here a concentration of 100% milk corresponds to the milk as it is when opening a sealed package and lower concentrations also used in the measurements of the milk (0%, 25%, 50% and 75%) are defined as the ratio of milk to water, where the milk is diluted by adding water. The special case of 0% milk corresponds to a sample only containing water. For each sample the fiber and detector position were kept constant and the milk had to be on the same level in the package not to affect the results. As shown before, slight deviations in fiber position is allowed without affecting the outcome of the measurement, as is shown in Table 5.1. However, keeping a constant level on the liquid in the package is crucial, as a change will directly result in a longer or shorter path that the light can travel.

The results of the measurements on different milk concentrations yielded that for higher concentrations of milk, an increase in intensity could be observed. This means that for higher concentration of milk which gives a higher scattering coefficient of the liquid, more photons have the possibility to escape the surface of the liquid by backscattering and then reach the detector. For increasing milk concentrations we can also observe a decrease in the mean total optical path length and an increase in absorption path length. This is also related to the increased scattering in the liquid.

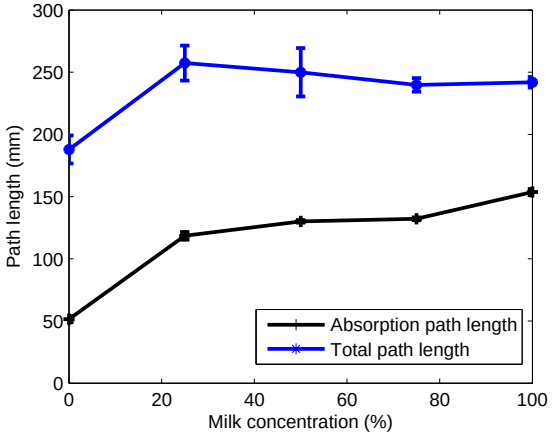

Figure 5.4: Oxygen absorption path length (black) and mean optical path length (blue line). The mean optical path length is calculated for three different modulation frequencies and different milk concentrations are obtained by diluting the milk in water. A milk concentration of 0% corresponds to only water.

When the scattering is increased, the light will backscatter closer to the surface and light penetrating deeper into the liquid will not, due to the scattering, be able to escape back into the headspace and be detected. This phenomenon will reduce the total path length, but for the same reason the absorption path length will instead increase, because when light is escaping from the liquid it will when detected have taken a longer path through the air and give an increasing contribution to the absorption signal. However, a drastic drop in both the absorption path length and total path length is observed when the milk is replaced by water. Now we have much less scattering compared to milk and light propagating into the liquid will have a very small probability to be backscattered up into the headspace and be detected, thus giving both a decrease in absorption and total path length.

This study shows that because of scattering inside the milk, the combination methods can be used to retrieve information on the optical properties in the liquid. However, it is not, as in the previous section, as easy to relate the total optical path length to the absorption path length, and calibration is needed where the milk has to be taken into account.

5.1.4 Bacterial growth studies in a milk package

A sealed milk package, fresh from the fridge, was measured over several days. The source and detector was positioned as in previous measurement. The absorption signal was collected every 7 minute and the setup was switched to the FDPM mode 1-2 times a day to measure the total path length. The last 70 hours of the measurement sequence are shown in Figure 5.5. At the end of the measurement, the absorption signal had vanished. The depletion of oxygen occurs over a time period of roughly 15 hours. The uptake of oxygen from the milk is caused by aerobic bacteria, which after a set time become active and start to grow while consuming oxygen. The bacterial growth, which is an exponential increase in bacteria concentration, can be modelled with the so-called modified Gompertz equation [31]. It is an exponential function and it is modified in

such way that the parameters have a biological meaning.

$$c = A\left(1 - \exp\left(-\exp\left(\frac{\mu_m * 2.71}{A}(\lambda - t) + 1\right)\right)\right) \tag{5.4}$$

Here A is the maximum size of the population, μ_m is the maximum growth rate and λ is the lag time.

A modified Gompertz equation was, through the non-linear least-square method, fitted to the experimental data (Figure 5.5) using the statistical tools available in MATLAB. Values of the fitted parameters were, $A = 183$ mm, $\mu_m = 13$ mm/h and $\lambda = 32$ h. Here A is our maximum path length, μ_m is the value for the maximum derivative of the path length and λ the time at which the oxygen starts to decrease. In bacterial growth, three phases can be distinguished that are of relevance; the lag, log and stagnation phases. The lag phase corresponds to the time in which the bacteria have to adapt to its environment in order to start to grow and is not yet able to divide. The log phase starts after the lag phase, in which the bacteria grow at a constant rate, showing an exponential growth in population. After the log phase comes the stagnation phase in which the population stops to grow, which can be due to a depletion of nutrients or oxygen.

In this measurement only the decrease in oxygen is measured and not the bacterial population. However, research has been done which relates the oxygen and carbon dioxide concentration in vial headspaces to the bacteria concentration by using the modified Gompertz equation [32]. This means that the values on the parameters in Equation 5.4 could be used to relate to the actual bacterial population. A huge advantage with this measurement technique is that compared to conventional techniques for gas concentration evaluation, the GASMAS technique can measure continuously and is nonintrusive.

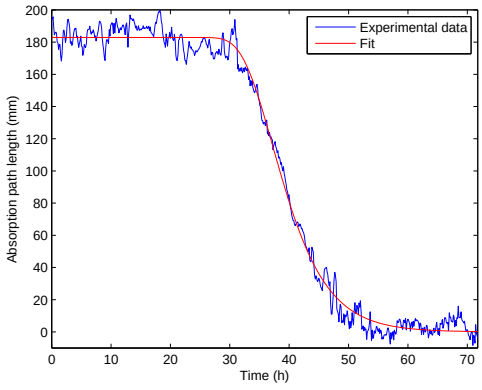

Figure 5.5: Absorption path length measured continously over time in a sealed milk package. It is fitted to the Gompertz equation.

The phase shifts measured by the FDPM technique did not change during the whole recording period, which indicates that the total path length did not change over time. The constant total path length shows that the scattering properties of the milk do not change substantially when the milk goes from fresh to spoiled, implying that the scattering properties of the spoiled milk are not significantly different from those

of the fresh milk. So the decrease in measured absorption path length is not because of changed optical properties in the milk, as was the case shown in Figure 5.4.

5.2 Gas diffusion in wood

To measure gas diffusion in wood samples, a probe was designed consisting of two optical fibers. One was coupled to the diode laser and the other one to the PMT. The fiber tips were inserted into wood samples, which had holes with a diameter of around 10 mm and depth of 6 cm drilled. The hole was then sealed as well as possible to ensure that no gas surrounding the wood sample seeps in. At a distance of 10 and 15 mm from the probe, holes were drilled with the same depth as the probe hole. The working principle was to flush with nitrogen in the test holes and through diffusion the nitrogen gas would reach the area around the probe. When the nitrogen pushes away the oxygen, it should be observed as a decrease in the gas absorption signal due to the oxygen.

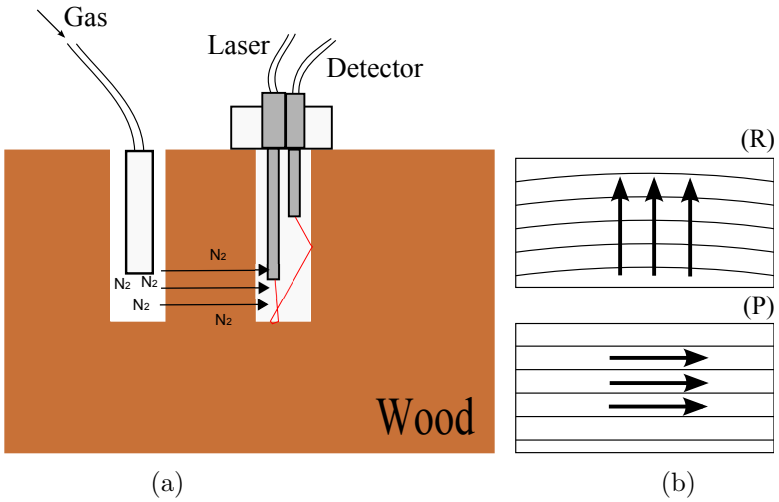

Figure 5.6: (a) Schematic figure of the setup when doing the gas diffusion measurements. At the left the nitrogen is flushed and later diffusing in to the right part where the fibers to the laser and detector are positioned. The distance between the holes in the wood samples were 10 and 15 mm (b) Gas diffusing radially (R) and parallel (P) to the tree ring lines are presented.

Wood samples from pine and mahogany were used in the measurements. As previously discussed, wood has an internal structure which has to be taken into consideration. Two different measurement geometries were employed, one in which the flushing gas had to diffuse parallel to the direction of the tree year ring lines and the other one in which the gas diffused radially to these lines (Figure 5.6). The two geometries were studied for both the pine and mahogany samples.

When performing the measurements and in order to be able to compare them, the flow of gas leaving the nozzle of the gas tube had to be kept constant. This was achieved by trying to keep a constant pressure at 2 bar from the gas bottle containing nitrogen. Before the gas is turned on, the gas absorption signal is measured in atmospheric conditions and the resulting WMS signal is then used as a reference measurement of

the absorption strength.

$$y = (1 - A) * e^{-t/T} + A \tag{5.5}$$

The samples were measured continuously over 30-80 minutes, with an integration time of 20 s for each measurement. The data are then normalized against normal atmospheric conditions and fitted to an exponential function (Equation 5.5). Here T is a time constant, characterizing the diffusion of nitrogen in the sample, translating to the oxygen being pushed away. A is the converging value, interpreted as when the system has reached an equilibrium.

From the measurements we could observe that the light colored pine sample gave a better absorption signal, and the more dark colored mahogany wood absorbed more light and a lower gas absorption signal was obtained. The time constant for the pine sample measured in the parallel configuration (P) showed similar behaviour when measured at 10 mm (T=3.9 min) and 15 mm (T = 4.0 min), but with larger difference in A, $A_{10mm} = 0.47$ and $A_{15mm} = 0.54$ (Figure 5.7). The gas absorption measured in radial configuration (R) at a distance of 10 mm from the probe showed little or none diffusion. When doing the same set of measurements in the mahogany wood, the P configuration showed a significant increase of the time constant with increasing distance of gas nozzle and probe, $T_{10mm,P} = 6.4$ min, $T_{15mm,P} = 28$ min, $A_{10mm,P} = 0.16$ and $A_{15mm,P} = 0.46$. The R configuration was similar to the corresponding measurement for the pine, with none or negligible decrease in the oxygen absorption signal.

There are several interesting remarks regarding the results from the gas diffusion measurements in the pine and mahogany sample. The first thing worth notice is that when the gas has to diffuse radially to the tree lines no diffusion is observed for either pine or mahogany, but when changing the geometry to diffusion parallel to the tree lines a very fast diffusion is observed for both wood samples at a 10 mm distance. This could be explained by the very anisotropic structure of the wood sample, as shown in Figure 4.3. When comparing different samples, it is also noticeable that the 10 mm measurement in P configuration shows a similar diffusion but the lower limits of the absorption signal (A value) are different. The process that defines the value of this equilibrium signal is how fast the diffusion out from the area around the probe is, relative to the diffusion in. For pine wood materials this means that we have both a fast diffusion into the probe and out, which results in a equilibrium with a significant oxygen concentration and a very fast exchange rate with ambient air. The diffusion in mahogany is much slower; the surrounded wood material acts more like a wall that is preventing fast gas exchange with ambient air. Thus, the equilibrium level of O_2 can be lowered by a slow nitrogen-injection process. This is demonstrated when the diffusion distance is increased to 15 mm; for the mahogany sample a much slower diffusion process is observed, while for the pine sample the diffusion and equilibrium concentration for 15 mm are similar to the values for 10 mm.

The gas diffusion studies show that this method could be employed on archaeological wood materials in order to obtain information about its structure. This could be a promising alternative method to circumvent the non-transmissive properties of archaeological wood which make it difficult to perform absorption spectroscopy.

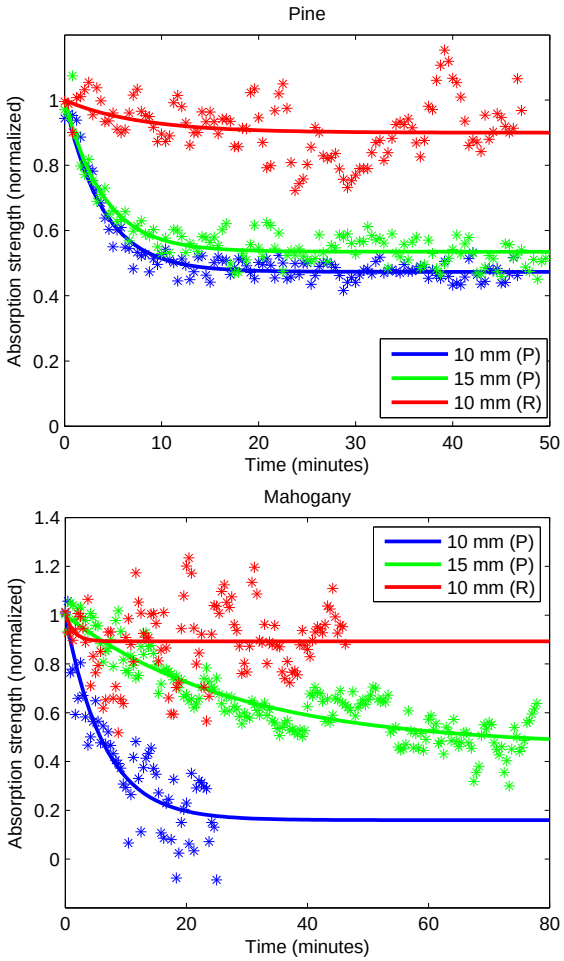

Figure 5.7: Top figure represents the gas diffusion measurements done in pine wood, for parallel (P) and radial (R) propagation of the nitrogen gas from gas nozzle to the probe. The propagation distance of the gas was measured for 10 and 15 mm. The figure at the bottom shows the same measurement done for diffusion in mahogany wood.

Chapter 6

Conclusions and Outlook

In this work, it has been demonstrated that it is possible to employ the combined method of the GASMAS and the FDPM techniques to monitor gas content in food packages. It is also shown that both the absorption path length and the total optical path length are dependent on the optical properties of the liquid inside the package. This prevents us from directly using the total optical path length as a measure of the absorption path length, but instead the total optical path length can be used for monitoring of changes of the optical properties in the liquid. Further investigations could be to measure on different kinds of liquids, such as juices. The previous knowledge about the total optical path length was then applied when doing the bacterial growth studies in a milk package. By observing no change in total optical path length it was concluded that the change in absorption signal arises from a change in oxygen concentration in the head space. The long-time measurement on the absorption path length in the food package was then fitted to a bacterial growth equation. This possibility of indirect measuring the bacterial population by using the GASMAS technique could serve as a powerful alternative to conventional methods which are destructive. Future studies could be to prepare samples with a certain bacteria culture and study the growth by using GASMAS. The bacterial growth could also be studied in more food packages, in both sealed and opened packages. Applying a second diode laser, the carbon dioxide concentration could also be simultaneously monitored together with the oxygen gas concentration.

The gas diffusion studies performed in pine and mahogany wood samples, by using a probe design, demonstrates that this could be a promising method for continued studies in wood materials. From the result we can observe a clear difference in diffusion properties between the pine and mahogany wood samples. Future studies should be to pursue the application of the fiber probe design to do gas diffusion measurements in archaeological wood materials, such as from the Vasa ship. With the probe it could be possible to do measurements on site at the Vasa ship, utilizing that it has already drilled holes from its construction. Other interesting studies could be to compare wet and dry wood or how the gas content inside the wood is affected when the wood sample is heated up, which are related to the wood drying process. In this work only nitrogen was used, but it could be interesting to flush with other gases such as carbon dioxide and oxygen to investigate if it is possible to observe different behaviors in the gas diffusion.

Chapter 7

Acknowledgements

I would like to express my great appreciation towards my supervisors Liang Mei and Sune Svanberg. Without their support, encouragement and inspiration, this thesis work would not have been possible. I would also like to thank Patrik Lundin for the support and the times we spent sharing the lab. Many thanks also go to Jan von Keitz, who I shared office and lab with, and I wish you the best of luck in your continued studies. I would like to thank the whole of Atomic Physics Division and feel very grateful for be able to do my project in such a helpful and stimulating environment. I would also like to give my appreciation to my former supervisor during my bachelor's project — Gabriel Somesfalean, who has been a great motivation for carrying out my master work in the Atomic Physics Division. Lastly, I would like to thank my family for showing support not only during my thesis work but throughout my whole physics education.

Chapter 8

Self-reflection

In this section I am going to discuss about the experience and personal development that I have obtained when doing my master project. When I started my master work at the beginning of the spring semester (2014) I had already done my bachelor degree in the same field. During the time in-between the two projects I took courses mainly related to optics and molecular physics. From this a great foundation was obtained when approaching the project.

Doing physics at a tabletop scale involves working a lot with electronics, an experience which is never really obtained by taking courses and are important skills that are developed during a diploma project. During the project, by working with a lot with the equipments one also learn how to work more fluidly in the lab, which also increase the capacity of working individually. By also doing a full time project I would say one obtain a better insight on how it is to work in a research environment and to be more involved in various running projects. When doing my master work I had also the possibility to collaborate and discuss with others from other fields of physics and sciences, which made it possible to put the work I did into a wider perspective.

I also found that making a time plan at the beginning of the project helped out. Even if the plan was not followed completely it gave a feeling of how the work proceeded, which was helpful. To be self-critical I would probably prefer to start even earlier on writing my thesis, even though that I had a first draft ready for the mandatory half-time meeting. Except from only working in the lab, I also performed data analysis and prepared the samples. For literature studies I focused on studying some of the theory behind wavelength modulation spectroscopy and previous research done on wood materials and food packages, not only in the field of physics but also in other fields such as biology and chemistry. This provided an insight into how the problems were solved by other non-optical and optical techniques. It was also very fun to be working with the PhD students in the group and during my time they both had their dissertations, which were interesting to follow. Overall I would say that my project went well, of course there is always room for improvements, such as having more results to present but that is also one challenge when doing this kind of applied physics. It is very difficult to predict the expected results of measurements, so sometimes one have to play around with samples. For example, when we measured on wood materials. One idea before the diffusion measurements was to measure the backscattering in the wood by having the detector and laser in a reflective geometry, and then just put the system in water to see if we could observe the water diffusing into the wood. Difficulties in recording a good enough absorption signal had us to further investigate possible

measurement geometries, which would then result in the probe measurements.

To conclude this section, I would like to think that my scientific skills have been improved during this project and I am looking forward to further develop them. It will also be interesting to see what further studies of the topics presented in this thesis will yield.

Bibliography

[1] Y. Kambe, Y. Yoshii, K. Takahashi, and K. Tonokura. Monitoring of atmospheric nitrogen dioxide by long-path pulsed differential optical absorption spectroscopy using two different light paths. *Journal of Environmental Monitoring*, 14(3):944–950, 2012.

[2] N. C. Zeitouni, A. D. Paquette, J. P. Housel, Y. Shi, G. E. Wilding, T. H. Foster, and B. W. Henderson. A retrospective review of pain control by a two-step irradiance schedule during topical ALA-photodynamic therapy of non-melanoma skin cancer. *Lasers in Surgery and Medicine*, 45(2):89–94, 2013.

[3] A. Nevin, G. Spoto, and D. Anglos. Laser spectroscopies for elemental and molecular analysis in art and archaeology. *Applied Physics A-Materials Science & Processing*, 106(2):339–361, 2012.

[4] Z. S. Li, J. Kiefer, J. Zetterberg, M. Linvin, A. Leipertz, X. S. Bai, and M. Alden. Development of improved PLIF CH detection using an alexandrite laser for single-shot investigation of turbulent and lean flames. *Proceedings of the Combustion Institute*, 31:727–735, 2007.

[5] M. Sjöholm, G. Somesfalean, J. Alnis, S. Andersson-Engels, and S. Svanberg. Analysis of gas dispersed in scattering media. *Optics Letters*, 26(1):16–18, 2001.

[6] M. Lackner. Tunable diode laser absorption spectroscopy (TDLAS) in the process industries - a review. *Reviews in Chemical Engineering*, 23(2):65–147, 2007.

[7] J. Larsson. *Development of a spectroscopic technique for assessment of optical properties and gas content in porous turbid media -application to wood.* Bachelor thesis, Department of Physics, Lund University, 2012.

[8] L. Mei, J. Larsson, S. Svanberg, and G. Somesfalean. Optical porosimetry in wood using oxygen absorption spectroscopy and frequency domain photon migration. In *2012 Asia Communications and Photonics Conference (ACP)*, 2012.

[9] L. Mei, S. Svanberg, and G. Somesfalean. Combined optical porosimetry and gas absorption spectroscopy in gas-filled porous media using diode-laser-based frequency domain photon migration. *Optics Express*, 20(15):16942–16954, 2012.

[10] M. Born and R. Oppenheimer. Zur quantentheorie der molekeln. *Annalen der Physik*, 389:457–484, 1927.

[11] J.N. Murrell. The origins and later developments of molecular orbital theory. *International Journal of Quantum Chemistry*, 112(17):2875 – 2879, 2012.

[12] M. Planck. Ueber das Gesetz der Energieverteilung im Normalspectrum. *Annalen der Physik*, 309:553–563, 1901.

[13] A. Einstein. Uber einen die Erzeugung und Verwandlung des Lichtes betreffenden heuristischen Gesichtspunkt. *Annalen der Physik*, 322:132–148, 1905.

[14] A. B. Kostinski. On the extinction of radiation by a homogeneous but spatially correlated random medium. *Journal of the Optical Society of America A -optics image science and vision*, 18(8):1929 – 1933, 2001.

[15] J. Heino, S. Arridge, J. Sikora, and E. Somersalo. Anisotropic effects in highly scattering media. *Physical Review E - Statistical, Nonlinear, and Soft Matter Physics*, 68(3 1):319081–319088, 2003.

[16] D. Gorpas and S. Andersson-Engels. Evaluation of a radiative transfer equation and diffusion approximation hybrid forward solver for fluorescence molecular imaging. *Journal of Biomedical Optics*, 17(12), 2012.

[17] B.T. Wong and M.P. Mengu. A unified monte carlo treatment of the transport of electromagnetic energy, electrons, and phonons in absorbing and scattering media. *Journal of Quantitative Spectroscopy and Radiative Transfer*, 111(3):399 – 419, 2010.

[18] R.N. Hall, G.E. Fenner, J.D. Kingsley, T.J. Soltys, and R.O. Carlson. Coherent light emission from GaAs junctions. *Physical Review Letters*, 9(9):366–368, 1962.

[19] Zhores I Alferov. Semiconductor devices with heterojunctions. *Soviet Physics Uspekhi*, 15(6):834, 1973.

[20] E.D. Hinkley. High-resolution infrared spectroscopy with a tunable diode laser. *Applied Physics Letters*, 16(9):351 – 354, 1970.

[21] L. Zhang, F. Wang, J. Yan, and K. Cen. NO concentration sensing at 1.79 µm transition using tunable diode laser absorption spectroscopy. *AIP Conference Proceedings*, 1592:254 – 260, 2014.

[22] Q. Gao, Y. Zhang, J. Yu, S. Wu, Z. Zhang, Fu. Zheng, X. Lou, and W. Guo. Tunable multi-mode diode laser absorption spectroscopy for methane detection. *Sensors and Actuators A (Physical)*, 199:106 – 110, 2013.

[23] C.A. Rice, K.C. Gross, and G.P. Perram. Investigation of atmospheric $O_2 X^3\Sigma_g^-$ to $b^1\Sigma_g^+$ using open-path tunable diode laser absorption spectroscopy. *Applied Physics B: Lasers and Optics*, 111(2):173 – 182, 2013.

[24] Y. He, Y. Zhang, L. Wang, K. You, Y. G, A. Zhu, and W. Yang. An ammonia sensor with high sensitivity in farmland based on laser absorption spectroscopy technology. In *Proceedings of the SPIE - The International Society for Optical Engineering*, volume 8561, page (7 pp.), 2012.

[25] U. Tylewicz, P. Rocculi, P. Lundin, L. Cocola, S. Svanberg, K. Dymek, P. Dejmek, and F. Gomez Galindo. Gas in scattering media absorption spectroscopy (GASMAS) detected persistent vacuum in apple tissue after vacuum impregnation. *Food Biophysics*, 7(1):28–34, 2012.

[26] L. Mei, G. Somesfalean, and S. Svanberg. Optical characterization of micro-porous ceramics using tunable diode laser. In *Proceedings of the SPIE - The International Society for Optical Engineering*, volume 8570, page (6 pp.), 2013.

[27] P Kluczynski, J Gustafsson, AM Lindberg, and O Axner. Wavelength modulation absorption spectrometry - an extensive scrutiny of the generation of signals. *Spectrochimica Acta Part B-Atomic Spectroscopy*, 56(8):1277 – 1354, 2001.

[28] R. R. Rangaprasad. Modified atmospheric packaging (MAP) technology for fruits and vegetables – an overview. *Popular Plastics & Packaging*, 59(1):35 – 37, 2014.

[29] J. Iejavs and U. Spulle. Structural properties of cellular wood material. *Pro Ligno*, 9(4):491 – 497, 2013.

[30] M. Andersson, L. Persson, M. Sjöholm, and S. Svanberg. Spectroscopic studies of wood-drying processes. *Optics Express*, 14(8), 2006.

[31] M. H. Zwietering, I. Jongenburger, F. M. Rombouts, and K. Vantriet. Modeling of the bacterial-growth curve. *Applied and Environmental Microbiology*, 56(6):1875–1881, 1990.

[32] A. Bevilacqua, M. R. Corbo, G. Martino, and M. Sinigaglia. Evaluation of pseudomonas spp. through O_2 and CO_2 headspace analysis. *International Journal of Food Science and Technology*, 48(8):1618–1625, 2013.